

Integration of Interactive Corrections to Model-Based Segmentation Algorithms

Holger Timinger^{1,2}, Vladimir Pekar¹, Jens von Berg¹
Klaus Dietmayer² and Michael Kaus¹

¹Philips Research Laboratories, Division Technical Systems,
Roentgenstrasse 24-26, 22335 Hamburg

²Department of Measurement, Control and Microtechnology,
University of Ulm, Albert-Einstein-Allee 41, 89081 Ulm
Email: holger.timinger@philips.com

Abstract. 3D deformable shape models have become a common approach for solving complex segmentation tasks in medical image processing. Nevertheless sometimes the segmentation fails due to low image resolution or contrast, structures lying closely together or an insufficient initialization of the model. Although the error is often obvious to physicians, they have no opportunity to improve the result. This paper presents 3D tools for the correction of erroneous segmentations and provides a method which allows the integration of these corrections to deformable model-based segmentation methods. The integration is accomplished by a user deformation energy which is defined in a way that allows efficient corrections without the need to segment the complete erroneous region manually. This new approach is illustrated on the segmentation of a vertebra and a femur-head.

1 Introduction

Segmentation of 3D medical images is a prerequisite for many image analysis tasks. Commonly the segmentation is done manually in 2D cutplanes. This is time consuming and the results are of limited reproducibility. Therefore much work has been done in order to develop automated segmentation algorithms. For this, deformable models have become a promising approach. Kass et al.[1] developed 2D deformable models called snakes. Cootes and Taylor[2] presented more advanced models based on statistical evaluation. Weese et al.[3] combined Cootes statistical models and 3D deformable shape models and embedded them into a common adaptation framework. Despite the improvements in modeling anatomic structures and in segmentation algorithms, errors in the segmentation sometimes remain, e.g. due to structures lying closely together. In order to circumvent errors in the segmentation result some approaches try to integrate the user input to the segmentation process. Olabarriaga and Smeulders [4] summarize and rate some approaches which are based on e.g. modifying global

parameters or pictorial input. Neither corrections based on restarting the adaptation nor accurate interactions improve performance significantly. The latter one would require similar effort as slice-wise contouring. In this paper we present a new approach where the user can adjust 3D deformable models efficiently. In addition we prove the accuracy of the new methods.

2 Methods

2.1 Model-Based Segmentation

The approach for interactive segmentation presented in this paper is based on an automated model-based segmentation process [3] with 3D shape models. The shape model is represented by a triangular mesh and can be defined as follows

$$\tilde{\mathbf{m}} \approx \bar{\mathbf{m}}^0 + \sum_{k=1}^M p_k \cdot \mathbf{m}^k, \quad (1)$$

where $\bar{\mathbf{m}}^0$ is the mean shape model, \mathbf{m}^k are the modes of the model, p_k the corresponding weights and M is the total number of modes. During the segmentation process, this model is adapted iteratively to the anatomic structure within the image. The adaptation iterates two steps. In the first step, the potential surface of the anatomic structure within the image data is detected. The search is performed along the triangle normal \mathbf{n}_i to find the point $\tilde{\mathbf{x}}_i$ with the optimal combination of feature value $F(\tilde{\mathbf{x}}_i)$ and distance δj to the triangle center $\hat{\mathbf{x}}_i$

$$\tilde{\mathbf{x}}_i = \hat{\mathbf{x}}_i + \mathbf{n}_i \delta \arg \max_{j=-l, \dots, l} \{ F(\hat{\mathbf{x}}_i + \mathbf{n}_i \delta j) - D \delta^2 j^2 \}, \quad (2)$$

where l is the search profile length and D controls the weighting of the distance and the feature value. The feature value is defined as

$$F(\mathbf{x}_i) = \pm \frac{g_{max} \cdot (g_{max} + \|\mathbf{g}_i\|)}{g_{max}^2 + \|\mathbf{g}_i\|^2} \cdot \mathbf{n}_i^T \cdot \mathbf{g}_i, \quad (3)$$

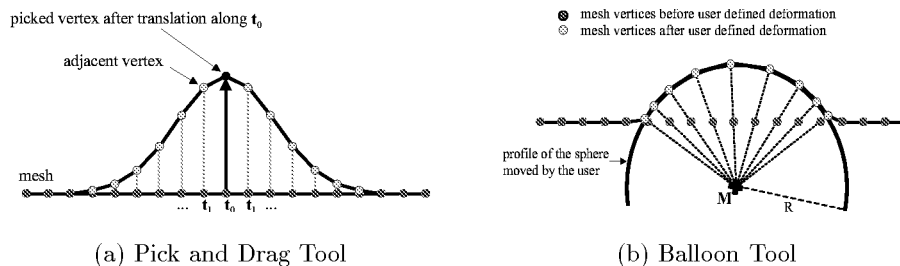
where \mathbf{g}_i is the image gradient at \mathbf{x}_i and g_{max} is a threshold in order to normalize $F(\mathbf{x}_i)$. This feature was optimized for bones in CT data [3]. After surface detection an energy which consists of an external and a weighted internal energy term $E = E_{ext} + \alpha \cdot E_{int}$ is minimized in the second step. The external energy drives the surface of the mesh towards the surface of the structure of interest

$$E_{ext} = \sum_{i=1}^T w_i \cdot (\tilde{\mathbf{x}}_i - \hat{\mathbf{x}}_i)^2, \quad w_i = \max \{ 0, F(\tilde{\mathbf{x}}_i) - D(\tilde{\mathbf{x}}_i - \hat{\mathbf{x}}_i)^2 \}, \quad (4)$$

where T is the number of triangles in the mesh and w_i is a weighting factor. The internal energy is designed to maintain the consistent distribution of the mesh vertices:

$$E_{int} = \sum_{i=1}^V \sum_{j=1}^{N(i)} \left(\mathbf{x}_i - \mathbf{x}_j - s \mathbf{R} \left(\mathbf{m}_i^0 - \mathbf{m}_j^0 + \sum_{k=1}^M p_k (\mathbf{m}_i^k - \mathbf{m}_j^k) \right) \right)^2, \quad (5)$$

Fig. 1. 2D principle of two different 3D tools for user defined mesh deformation.



where V is the number of vertices of the mesh, $N(i)$ is the number of neighbors of the vertex \mathbf{x}_i , s is the scaling, \mathbf{R} is the rotation and \mathbf{m}_i^0 , p_k and \mathbf{m}_i^k are the parameters of the statistical model according to eq. 1.

2.2 Interactive Segmentation

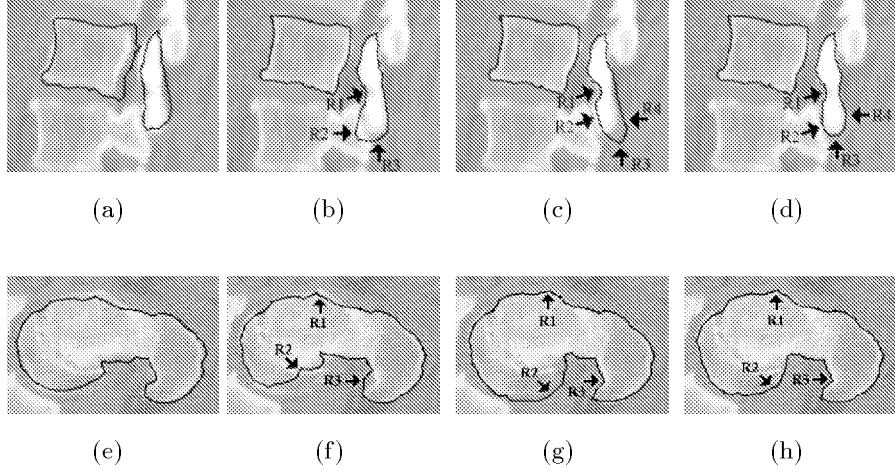
The presented automated segmentation algorithm shows good results especially for bone structures like spinal vertebrae [3]. However in some cases errors may occur when image resolution or contrast is low, anatomic structures lie close to each other or the model is insufficiently initialized. In order to adjust regions in which the automated segmentation algorithm fails, user interaction is necessary. In the subsequent section interaction tools are presented which allow efficient user defined deformations of the mesh in order to adjust it. These deformations can be integrated to the existing segmentation algorithm by defining an additional user deformation energy. This energy models the user defined deformation in a way that ensures accurate results even with corrections performed roughly.

3D Deformation Tools: Two basic tools have been designed for 3D user defined deformation of the mesh. The first tool is called *Pick & Drag Tool*. Its properties are visualized in fig. 1(a). The user picks a vertex of the mesh with the mouse and drags it to its new position. This translation can be described by the vector \mathbf{t}_0 . All neighbors of degree $k \in [1..k_{max}]$ of the picked vertex will be moved along the vector \mathbf{t}_k according to eq. 6:

$$\mathbf{t}_k = \mathbf{t}_0 \cdot e^{-\frac{1}{2} \cdot \left(\frac{w-k}{k_{max}}\right)^2}, \quad (6)$$

where w determines the dimensions of the deformation. The second tool is called *Balloon Tool*, see fig. 1(b). The user moves a sphere within the image. All vertices of the mesh which lie within the sphere are projected onto the surface of the sphere.

User Deformation Energy: Using the tools presented above means dropping out of the minimum of the energy term. Hence the user defined deformations could be partially reversed by the adaptation algorithm. In order to

Fig. 2. 2D cut of a 3D segmentation of a vertebra and a femur.

prevent the mesh from falling back into its previous state an additional energy term called user deformation energy E_{user} is introduced which models the user defined deformations. The aim of this approach is to circumvent the need to segment the image data exactly. The idea is that the user drags the erroneously segmented region of the mesh only very coarsely to the correct position, i.e. away from the local minimum, and then the automated segmentation algorithm will do the fine adjustment. In order to meet these requirements the energy which has to be minimized during the segmentation process is extended to $E = E_{ext} + \alpha E_{int} + \beta E_{user}$. The new user deformation energy E_{user} is defined as follows:

$$E_{user} = \sum_{triangles\ i} c_i \cdot (\hat{\mathbf{x}}_i - \hat{\mathbf{x}}_i^d)^2, \quad (7)$$

where $\hat{\mathbf{x}}_i$ is the triangle center deformed by the user, $\hat{\mathbf{x}}_i^d$ refers to the same triangle with the coordinates after user deformation and $c_i = \max\{0, F(\hat{\mathbf{x}}_i^d)\}$ is a weighting factor with $F(\hat{\mathbf{x}}_i^d)$ as in eq. 3. With this definition of c_i , energy components corresponding to triangles near the surface of anatomic structures will be weighted much stronger than components corresponding to triangles positioned elsewhere.

3 Results

In this section two examples are presented demonstrating the effects which can be accomplished by a single user interaction step. The adaptation is done using the same parameter values as in [3] and $\beta = 0.01$. For quantitative evaluation the mean square error (MSE) of the mesh triangles with respect to a manually performed reference segmentation has been calculated. Fig. 2(a) shows the mesh of

a vertebra in its initial position. The corresponding MSE is 1.20mm per triangle. In fig. 2(b) one can see the adapted mesh after 20 iterations (MSE 0.60mm). The regions R1-R3 are not segmented well and R2 adapted to an adjacent vertebra. In order to correct the error the user simply dragged the lower end of the mesh from the adjacent vertebra to the vertebra of interest and therefore out of a local minimum, see fig. 2(c) (MSE 0.58mm). R1 and R2 are now near the surface of the vertebra. R3 and R4 were shifted a bit too far. After 10 more iterations all regions R1-R4 are adapted accurately as one can see in fig. 2(d) and the final MSE decreased to 0.46mm. The adaptive weighting of the components of the user deformation energy forces R1 and R2 to stay at the surface of the vertebra and allows R3 and R4 to adapt to the surface as well. The same evaluation has been done for a femur. Fig. 2(e) shows the initial position of the mesh (MSE 1.00mm). After 20 iterations, see fig. 2(f), the MSE decreased to 0.66mm, but there are still regions R1-R3 that are not segmented perfectly. Fig. 2(g) depicts the mesh after user defined deformation (MSE 0.50mm) and fig. 2(h) shows the mesh after 10 more iterations with a final MSE of 0.40mm.

4 Discussion and Conclusion

The deformation tools presented in this paper enable corrections which allow the user to adjust regions of a mesh within a few steps. The user deformation energy models these corrections including also image information. Thus the user has to perform only coarse deformations which are refined by a subsequent automated adaptation. Further improvements can be made by developing sophisticated visualization tools in order to enhance the navigation of the deformation tools within the image. This extended segmentation algorithm may help to increase the acceptance of automated segmentations in daily clinical application because now segmentation is more robust and it is possible to interact with the algorithm.

5 Acknowledgement

We thank Prof. Dr. W. Mali, Prof. Dr. B. Eikelboom and Dr. J. Blankensteijn (Univ. Hospital Utrecht) for providing the images with the vertebrae and Dr. J. Richolt, Dr. J. Kordelle (Brigham & Women's Hospital) for the femur data.

References

1. M. Kass, A. Witkin, D. Terzopoulos. Snakes: active contour models. *1st ICCV*, pages 259–268, London, GB, 1987
2. T. Cootes, C. Taylor. Active Shape Models – Smart Snakes. In *BMVC*, pages 276–285, 1992.
3. J. Weese, M.R. Kaus, C. Lorenz et al. Shape Constraint Deformable Models for 3D Medical Image Segmentation. In *Proc. of IPMI*, pages 380–387, USA, 2001.
4. S.D. Olabariaga, A.W.M. Smeulders. Interaction in the Segmentation of Medical Images: A Survey. *Medical Image Analysis*, 5:127-142, 2001.